The analysis of complex behaviours of a novel three dimensional autonomous system*

Dong Gao-Gao(董高高)†, Zheng Song(郑 松), Tian Li-Xin(田立新),
Du Rui-Jin(杜瑞瑾), and Sun Mei(孙 梅)

Research Center for Nonlinear Science, Faculty of Science, Jiangsu University, Zhenjiang 212013*, China*

(Received 13 August 2009; revised manuscript received 25 January 2010)

This paper introduces a new three dimensional autonomous system with five equilibrium points. It demonstrates complex chaotic behaviours within a wide range of parameters, which are described by phase portraits, Lyapunov exponents, frequency spectrum, etc. Analysis of the bifurcation and Poincaré map is used to reveal mechanisms of generating these complicated phenomena. The corresponding electronic circuits are designed, exhibiting experimental chaotic attractors in accord with numerical simulations. Since frequency spectrum analysis shows a broad frequency bandwidth, this system has perspective of potential applications in such engineering fields as secure communication.

Keywords: three dimensional autonomous system, chaotic attractor, electronic circuit, frequency spectrum

PACC: 0545, 0547

1. Introduction

Over the last two decades, chaos analysis and applications have been studied extensively within many fields such as nonlinear circuits, secure communication, and economics. Since Lorenz discovered a simple three-dimensional smooth autonomous chaotic system in 1963, which has only two quadratic non-linearity terms, considerable research interests have been made in searching for the new chaotic attractors.[1,2] The Lorenz system, as the first chaotic model, revealed the complex and fundamental behaviours of the nonlinear dynamical system. In 2000, Chen and Ueta constructed a three-dimensional autonomous differential equation with only two quadratic terms, and found a new chaotic attractor in the study of anti-control of chaos (or, chaotification).[3] This new system was named Chen's system lately by others. Although this system seemingly has similar structure with the Lorenz system, they are not equivalent topologically. In fact, Chen system has been proved to be dual to the Lorenz system. However, theoretical analysis and numerical simulation suggested that the Chen's attractor has different topological structures from those of Lorenz system. Because of its complexity, the dynamical behaviours of Chen system have lately been carefully studied in the mathematics literatures and engineering machine. Both Lorenz system and Chen system possess a two-wing attractor. Afterwards, the stability and bifurcation of Chen system were analysed in Refs. [4] and [5]. The novel chaotic system which can generate more complex dynamic behaviours is very important in the field of chaotic theory and application. More recently, the generation of multi-scroll attractors seemed to be no longer a difficult task. Most of the methods were developed in literatures which shared some basic features: the multiple equilibriums were usually obtained by selecting nonlinearities with several breakpoints; the number of scrolls is equal to the equilibrium; the shape of the attractors is characterised by the fact that each scroll is a rotating cycle moving around the equilibrium point. According to the simple classification of three-dimensional (3D) autonomous chaotic systems with smooth quadratic terms presented by Lü *et al.*,[6,7] that is, from the viewpoint of the chaotic attractor solutions to the dynamical systems, one can clearly see an interesting fact: there are one-scroll attractors, two-scroll attractors and four-scroll attractors that have been found in the three-dimensional smooth quadratic autonomous

*Project supported by the National Natural Science Foundation of China (Grant No. 10771088), Natural Science Foundation of Jiangsu Province, China (Grant No. 2007098), Outstanding Personnel Program in Six Fields of Jiangsu Province, China (Grant No. 6-A-029), National Natural Science (Youth) Foundation of China (Grant No. 10801140), Youth Foundation of Chongqing Normal University, China (Grant No. 08XLQ04) and the Natural Science Foundation of the Jiangsu Higher Education Institutions of China (Grant No. 09B_202Z).

†Corresponding author. E-mail: gago999@126.com

© 2010 Chinese Physical Society and IOP Publishing Ltd

chaotic systems.[8−13] More recently, the generation of special attractors, multiple equilibriums and multiwing attractors seem to be more challenging topic. There are also novel 3D chaotic systems whose multiple equilibriums and amazing attractors are proposed in Refs. [14]–[18].

The outline of this paper is as follows: the 3D system is introduced in Section 2. Section 3 discusses the complex chaotic behaviour of novel system and complex dynamics by varying parameters e, h. Both Sections 4 and 5 discuss the electronic circuit and frequency spectra of novel system (1). Finally, the conclusion is given in Section 6.

2. A novel 3D chaotic system

2.1. Model

Considering the following novel 3D autonomous system:

$$\begin{aligned} \dot{x} &= axz - bx + cyz, \\ \dot{y} &= z + dy - exz, \\ \dot{z} &= fxy - gz - hx, \end{aligned} \tag{1}$$

here, x, y, z are state variables, a, b, c, d, e, f, g, $h \in R^+$ are constant parameters of the system (1).

2.2. Analysis of steady states

Here, let $a = 0.5$, $b = 1$, $c = 1$, $d = 4$, $e = 1.2$, $f = 1$, $g = 6$, $h = 0.1$, we discuss equilibria of this nonlinear system. Let $\dot{x} = \dot{y} = \dot{z} = 0$, the system has five equilibria, which are respectively described as follows:

$$\begin{aligned} S_1 &= (0, 0, 0), \\ S_2 &= (-4.1359, 3.7237, -2.4979), \\ S_3 &= (-3.9408, -1.5867, 1.1079), \\ S_4 &= (4.8524, -3.9191, -3.2504), \\ S_5 &= (5.0576, 1.5655, 1.2353). \end{aligned}$$

For equilibrium point $S_1 = (0, 0, 0)$, system (1) are linearised, the Jacobian matrix is defined as

$$\boldsymbol{J}_1 = \begin{bmatrix} az - b & cz & ax + cy \\ -ez & d & 1 - ex \\ fy - h & fx & -g \end{bmatrix} = \begin{bmatrix} -1 & 0 & 0 \\ 0 & 4 & 1 \\ -0.1 & 0 & -6.0 \end{bmatrix}.$$

To gain its eigenvalues, we let $|\lambda \boldsymbol{I} - \boldsymbol{J}_1| = 0$. These eigenvalues corresponding to equilibrium point $S_1 = (0, 0, 0)$ are respectively obtained as follows: $\lambda_1 = 4$, $\lambda_2 = -6$, $\lambda_3 = -1$. Here λ_1 is a positive real number, λ_2 and λ_3 are two negative real numbers. Therefore, the equilibrium point $S_1 = (0, 0, 0)$ is a saddle point. So this equilibrium $S_1 = (0, 0, 0)$ is unstable.

Next, linearising system (1) about the other equilibria such as S_2, S_3, S_4, S_5, we obtain the following characteristic operation. For equilibrium $S_2 = (-4.1359, 3.7237, -2.4979)$, the system (1) has a Jacobian matrix which is equal to:

$$\begin{aligned} \boldsymbol{J}_2 &= \begin{bmatrix} az - b & cz & ax + cy \\ -ez & d & 1 - ex \\ fy - h & fx & -g \end{bmatrix} \\ &= \begin{bmatrix} -2.2489 & -2.2489 & 1.6557 \\ 2.9975 & 4 & 5.9631 \\ 3.6237 & -4.1359 & -6.0000 \end{bmatrix}. \end{aligned}$$

We let $|\lambda \boldsymbol{I} - \boldsymbol{J}_2| = 0$. These eigenvalues correspond to the equilibrium $S_2 = (-4.1359, 3.7237, -2.4979)$ are $\lambda_1 = -6.5831, \lambda_2 = 1.1671 + 4.5444\mathrm{i}, \lambda_3 = 1.1671 + 4.5444\mathrm{i}$. Here λ_1 is a negative real number, λ_2, λ_3 become a pair of complex conjugate eigenvalues with positive real parts. The equilibrium S_2 is a saddle-focus point this equilibrium is unstable. For the same reason, we obtain the equilibrium $S_3 = (-3.9408, -1.5867, 1.1079)$, by calculation, we can obtain the eigenvalues of the Jacobian matrix of system (1), which are $\lambda_1 = -5.4480$, $\lambda_2 = 1.5010 + 3.0073\mathrm{i}$, $\lambda_3 = 1.5010 - 3.0073\mathrm{i}$, therefore, S_3 is an unstable saddle-focus point. We obtain the equilibrium $S_4 = (4.8524, -3.9191, -3.2504)$, by calculation, we can obtain the eigenvalues of the Jacobian matrix of the system (1) which are: $\lambda_1 = -6.9360$, $\lambda_2 = 1.1554 + 5.1014\mathrm{i}$, $\lambda_3 = 1.1554 - 5.1014\mathrm{i}$, therefore, S_4 is an unstable saddle-focus point. For equilibrium $S_5 = (5.0576, 1.5655, 1.2353)$, by calculation, we can obtain the eigenvalues of the Jacobian matrix of system (1), which are $\lambda_1 = -5.3499$, $\lambda_2 = 1.4838 + 3.4508\mathrm{i}$, $\lambda_3 = 1.4838 - 3.4508\mathrm{i}$, therefore, S_5 is an unstable saddle-focus point.

3. Numerical description of chaotic attractors

3.1. Typical phase portraits

When the parameters $a = 0.5, b = 1, c = 1, d = 4, e = 1.2, f = 1, g = 6, h = 0.1$ and ini-

tial condition $[0.4, 1, 0.4]$ are fixed, the corresponding Lyapunov exponents $L_1 = 0.0673 > 0; L_2 = -0.1561 < 0; L_3 = -7.2114 < 0$. Under the same condition, the corresponding Lyapunov dimension of chaotic attractors of this nonlinear-system is of fractional dimension, it is described as $D_{\rm L} = j + 1/|\lambda_{{\rm L}j+1}| \sum_{i=1}^{j} \lambda_{{\rm L}j} = 2 + (\lambda_{\rm L1} + \lambda_{\rm L2})/|\lambda_{{\rm L}j+1}| = 2 + (0.0673 - 0.1561)/|-3.1450| = 1.9718$, the Lyapunov dimension of this system is fractional. The fractal nature of an attractor does not merely mean that this system has non-periodic orbits, it also causes nearby trajectories to diverge. As all strange attractors, orbits that are initiated from different initial conditions soon reach the attracting set, but two nearby orbits do not stay close to each other, they soon diverge and follow utterly different trajectories in the attractor. Therefore, there are really strange chaotic attractors in this system. Under the same condition, the system (1) has chaotic attractor, Figs. 1(a), 1(b), 1(c) and 1(d), show x–y–z, x–y, y–z, x–z phase portraits of novel chaotic attractor. The time series of chaotic attractor is shown in Fig. 1(e). By choosing the slightly different initial conditions $[0.4, 1, 0.4]$ and $[0.4, 1.0000001, 0.4]$, figure 1(f) shows the great difference as time goes on. Therefore, the chaotic system (1) exhibits high sensitive dependence on initial conditions.

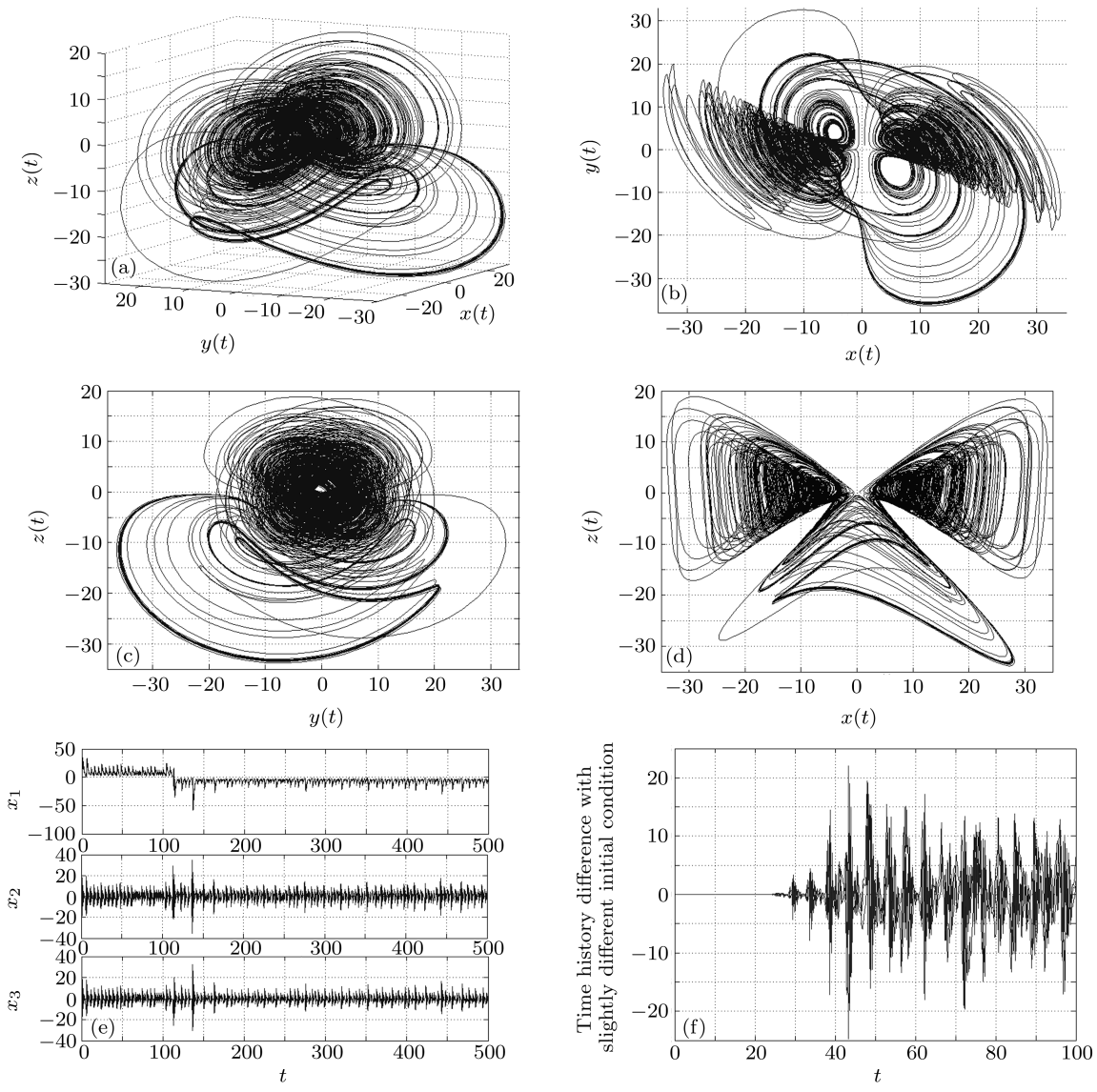


Fig. 1. (a) The 3D phase portrait of the chaotic attractor; (b) x–y phase portrait of chaotic attractor; (c) y–z phase portrait of chaotic attractor; (d) x–z phase portrait of chaotic attractor; (e) time series of chaotic attractor; (f) as time goes on, the greatly difference caused by slightly different initial conditions.

3.2. Varying parameter e

Many interesting complex dynamical behaviours have been founded by varying parameter e. As is well known, Lyapunov exponents measure the exponential rates of divergence or convergence of nearby trajectories in phase space. When parameters $a = 0.5, b = 0.6, c = 0.5, d = 4, f = 1, g = 6, h = 0.1$ and initial condition $[0.4, 1.2, 0.28]$ are fixed, as $e \in [0.48, 1]$, according to the detailed numerical as well as theoretical analysis, the Lyapunov exponents spectrum and maximum Lyapunov exponents spectrum are (L_1, L_2, L_3) shown in Fig. 2. The corresponding bifurcation diagram is also displayed in Fig. 3.

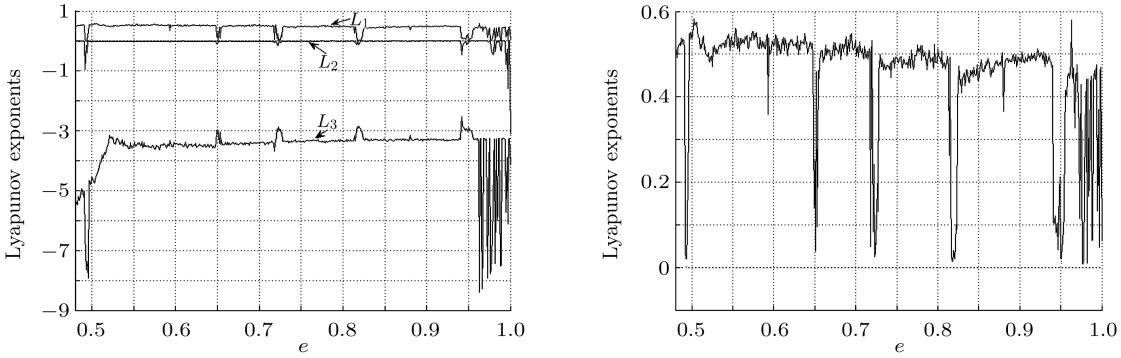


Fig. 2. Lyapunov exponents spectrum and maximum Lyapunov exponents spectrum varying with $e \in [0.48, 1]$.

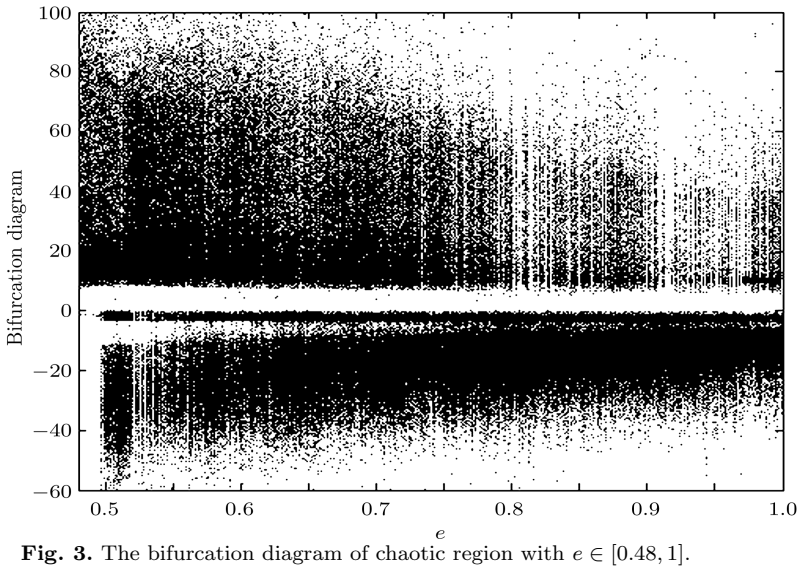


Fig. 3. The bifurcation diagram of chaotic region with $e \in [0.48, 1]$.

When the three Lyapunov exponents $L_1 > 0, L_2 < 0, L_3 < 0$, the system (1) is in chaotic state. From Figs. 2(a) and 2(b), $e \in [0.48, 1]$, the maximum Lyapunov exponents $L_1 > 0$, the system (1) is chaotic state. From Fig. 3, $e \in [0.48, 1]$, the bifurcation diagram shows that the system have complex chaotic dynamical behaviours. For example, as $e = 0.48$, the system (1) displays x–z and y–z chaotic portraits, as shown in Figs. 4(a) and 4(b). As $e = 0.5$, figures 4(c) and 4(d) show x–y–z and z–x phase portraits of chaotic attractor. As $e = 0.6$, system (1) shows x–y–z and x–z chaotic phase portraits, as shown in Figs. 4(e) and 4(f). As $e = 0.85$, figures 4(g) and 4(h) show x–y–z and x–z phase portraits of chaotic attractor. As an important technique, the Poincaré map is used to describe bifurcation and folding properties of chaos. As $e = 0.48$, we make $y = 0.8$ as crossing plane, the corresponding Poincaré map of the chaotic attractors is shown as Fig. 5(a). As $e = 0.5$, we make $y = 0.85$ as crossing plane the corresponding Poincaré map of the chaotic attractors is shown in Fig. 5(b). As $e = 0.6$, we make $z = 0.55$ as crossing plane, the corresponding Poincaré map of the chaotic attractors is shown in Fig. 5(c). As $e = 0.85$, we make $z = 0.45$ as crossing plane the corresponding Poincaré map of the chaotic attractor is shown in Fig. 5(d). From Figs. 5(a)–5(d), we can see that the system has extremely rich dynamical behaviours.

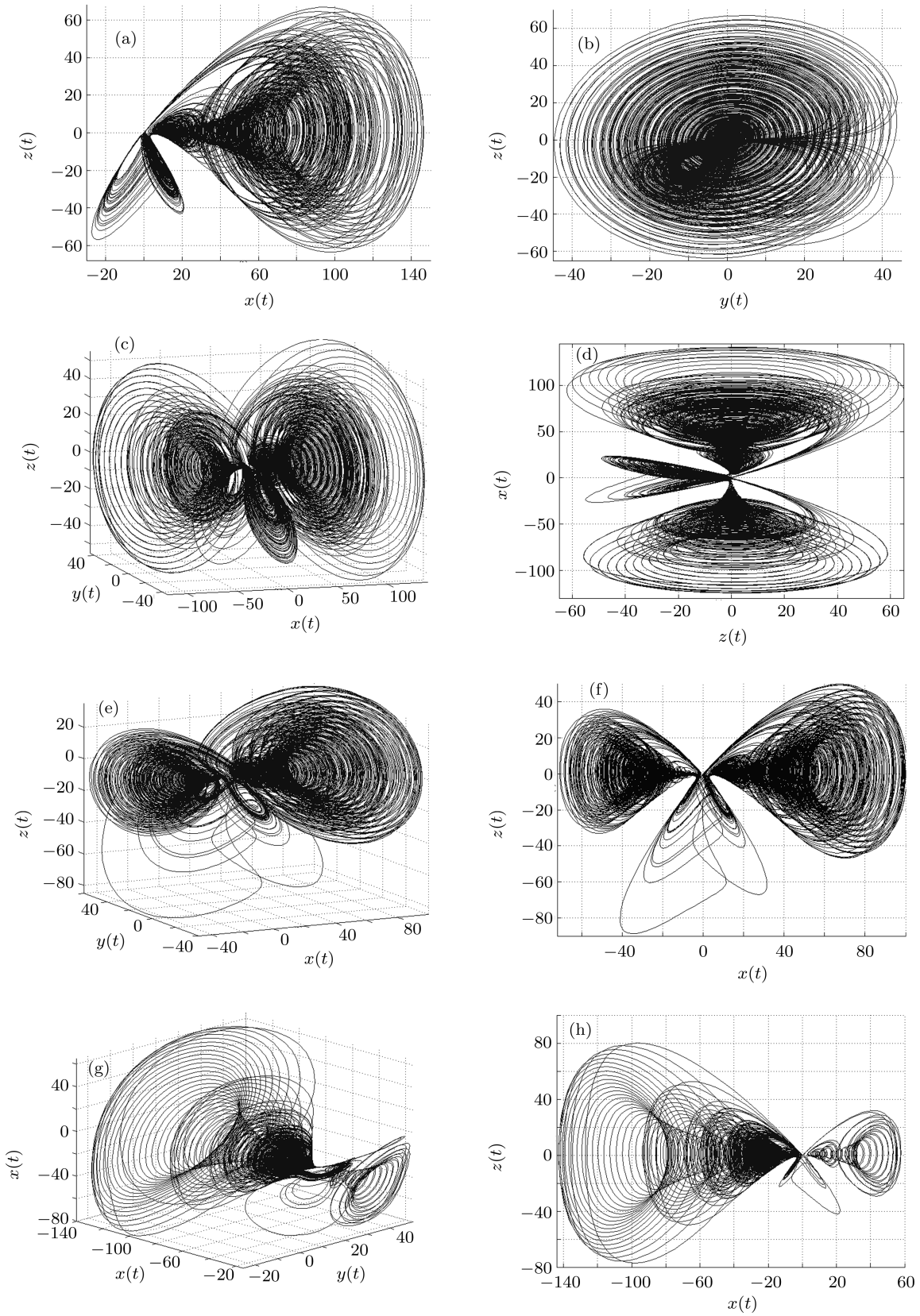


Fig. 4. (a) When $e = 0.48$, the x–z phase portrait of the chaotic attractor; (b) when $e = 0.48$, the y–z phase portrait chaotic attractor; (c) when $e = 0.5$, the x–y–z phase portrait of the chaotic attractor; (d) when $e = 0.5$, the z–x phase portrait chaotic attractor; (e) when $e = 0.6$, the x–y–z phase portrait of the chaotic attractor; (f) when $e = 0.6$, the x–z phase portrait chaotic attractor; (g) when $e = 0.85$, the x–y–z phase portrait of the chaotic attractor; (h) when $e = 0.85$, the x–z phase portrait chaotic attractor.

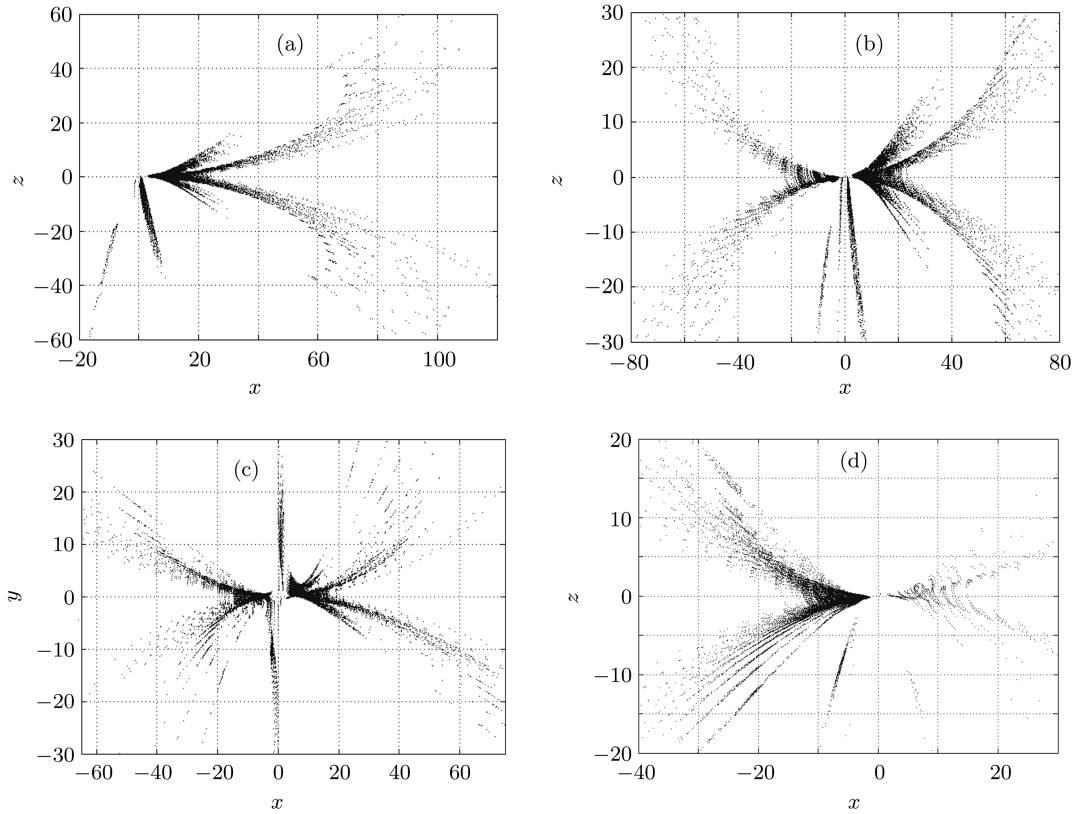


Fig. 5. (a) Projection on $x-z$ of the Poincaré map with $e=0.48,\ y=0.8$ as crossing plane; (b) projection on $x-z$ of the Poincaré map with $e=0.5, y=0.85$ as crossing plane; (c) projection on $x-y$ of the Poincaré map with $e=0.6, z=0.55$ as crossing plane; (d) projection on x–y of the Poincaré map with $e=0.85, z=0.45$ as crossing plane.

3.3. Varying parameter h

In this section, we use numerical computing and basic bifurcation analysis to investigate the dynamical behaviours of system (1). The evolution processes of the system are analysed precisely by means of Lyapunov exponents spectrum, bifurcation diagram and phase portraits by varying the parameter h in system (1). When parameters $a=0.5, b=1, c=1, d=4, e=1.2, f=1, g=6$ and initial condition $[0.4, 1, 0.4]$ are fixed, as $h\in[0.01, 0.5]$, according to the detailed numerical as well as theoretical analysis, the Lyapunov exponents spectrum and maximum Lyapunov exponent spectrum (L_1, L_2, L_3) are shown in Fig. 6. The corresponding bifurcation diagram of variable x with respect to parameter h is also displayed in Fig. 7. It can be observed that the bifurcation diagram well coincides with the Lyapunov exponents spectrum. For $h\in[0.01, 0.22]$, system (1) has one postitive and two negative Lyapunov exponents, which implies the existence of chaotic attractors of the system (1). For example, when $h=0.01, 0.12, 0.15, 0.19$, three dimensional phase portraits and two dimensional portraits are shown in Figs. 8(a)–8(h). For $h\in[0.35, 0.5]$, system (1) has one zero and two negative Lyapunov

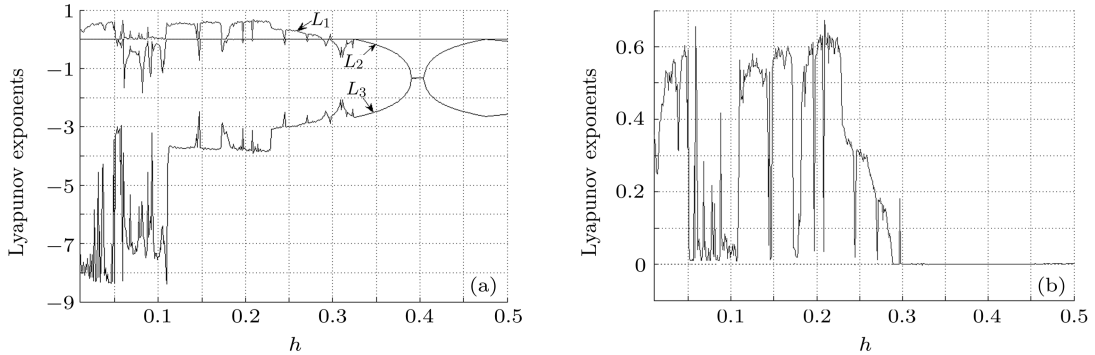


Fig. 6. Lyapunov exponents spectrum and maximum Lyapunov exponents spectrum varying with $h\in[0.01, 0.5]$.

exponents, which implies the periodic state of the system (1). For example, for $h = 0.35$, phase portraits of periodic state are shown in Figs. 8(i) and 8(j). As $h = 0.15$, we make $y = 0.55$ as crossing plane, the corresponding Poincaré map of the chaotic attractors is shown in Fig. 9(a). As $h = 0.19$, we make $z = 0.65$ as crossing plane the corresponding Poincaré map of the chaotic attractors is shown in Fig. 9(b).

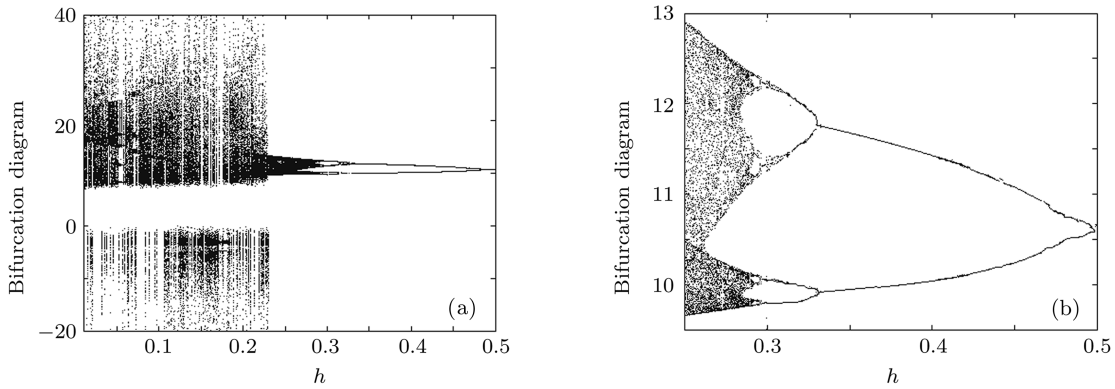
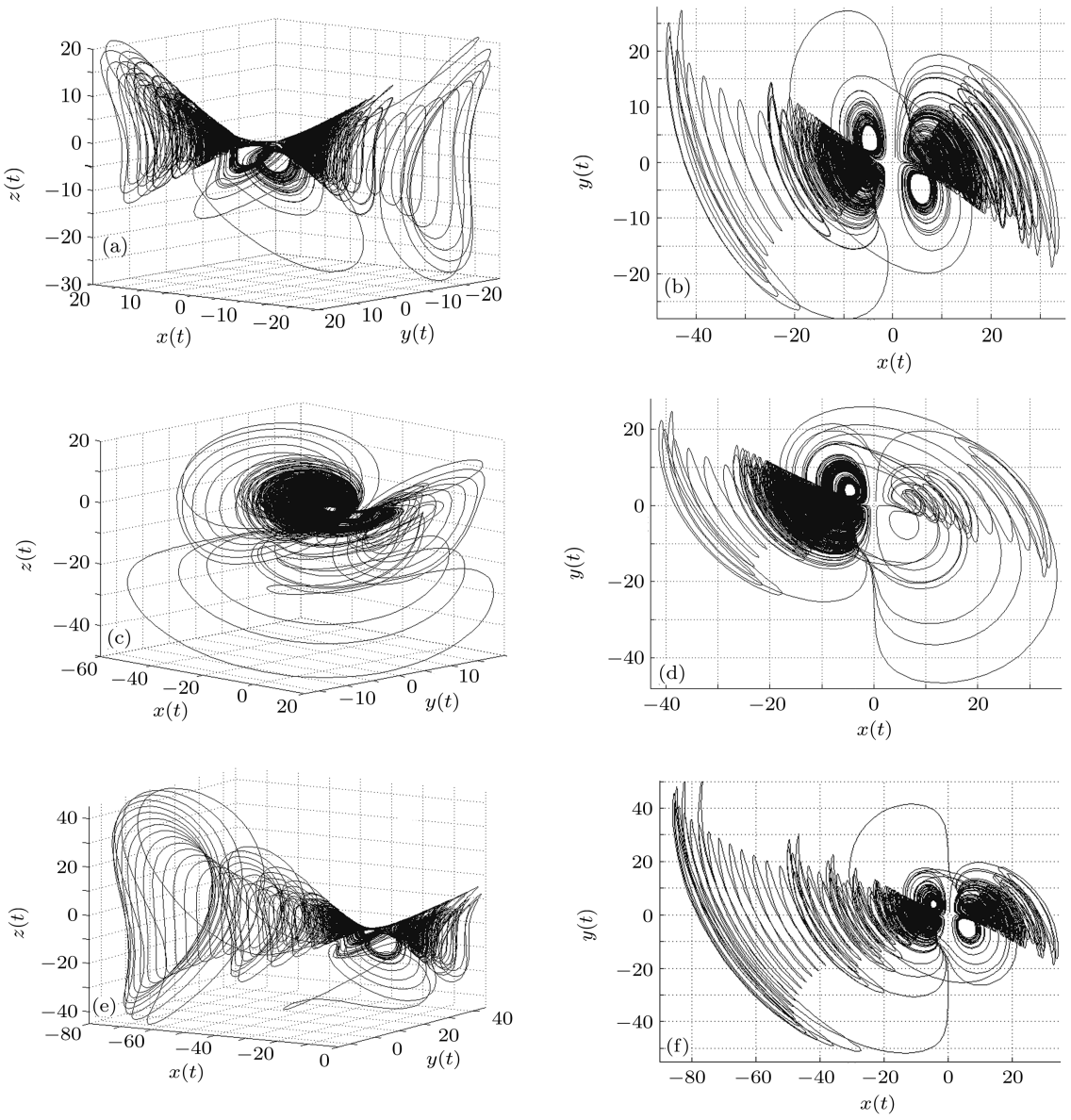


Fig. 7. The bifurcation diagram with $h \in [0.01, 0.5]$ and $h \in [0.25, 0.5]$.



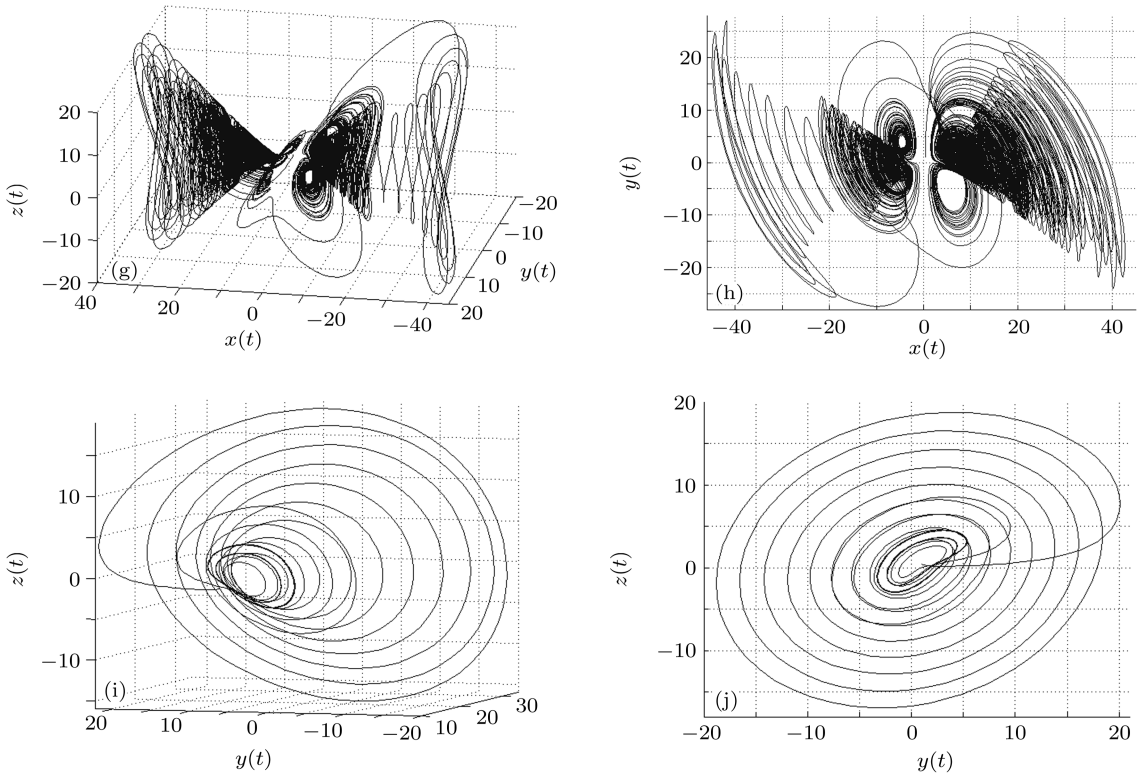


Fig. 8. (a) When $h = 0.01$, the $x - y - z$ phase portrait of the chaotic attractor; (b) when $h = 0.01$, the x–y phase portrait of the chaotic attractor; (c) when $h = 0.12$, the x–y–z phase portrait of the chaotic attractor; (d) when $h = 0.12$, the x–y phase portrait chaotic attractor; (e) when $h = 0.15$, the x–y–z phase portrait of the chaotic attractor; (f) when $h = 0.15$, the x–y phase portrait chaotic attractor; (g) when $h = 0.19$, the x–y–z phase portrait of the chaotic attractor; (h) when $h = 0.19$, the x–y phase portrait chaotic attractor; (i) when $h = 0.35$, the x–y–z phase portrait of periodic state; (j) when $h = 0.35$, the y–z phase portrait of periodic state.

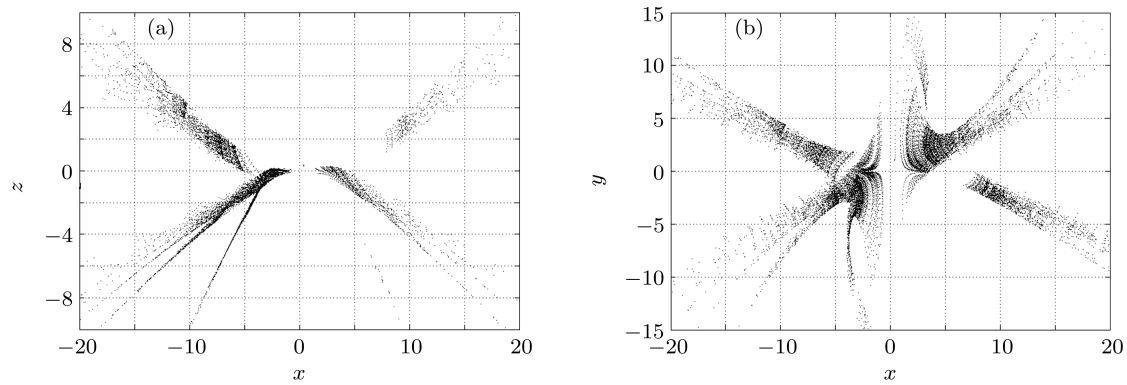


Fig. 9. (a) Projection on $x - z$ of the Poincaré map with $h = 0.15, y = 0.55$ as crossing plane; (b) projection on x–y of the Poincaré map with $e = 0.19$, $z = 0.65$ as crossing plane.

4. Circuit implementations

In this section, an electronic circuit is designed to physically realise the new chaotic system (1). The designed circuit of sytem (1) is shown in Fig. 10 based on Refs. [19]–[22]. The system (1) consists of three channels which realise that the three state variables x, y, z are transformed into $V_x = 100x, V_y = 100y, V_z = 100z$. The nonlinear terms in the equation are implemented linear resistors, linear capacitors, operational amplifiers and analog multipliers AD633. The scales of horizontal and vertical axes are 100 mV/div and 100 mV/div, the timebase is 0.50 ms/div respectively. All results were recorded from an oscilloscope of Multisim. Figure 11 shows phase portraits of x–y, y–x, x–z, y–z planes. The circuit experimental results show agreement with numerical simulations.

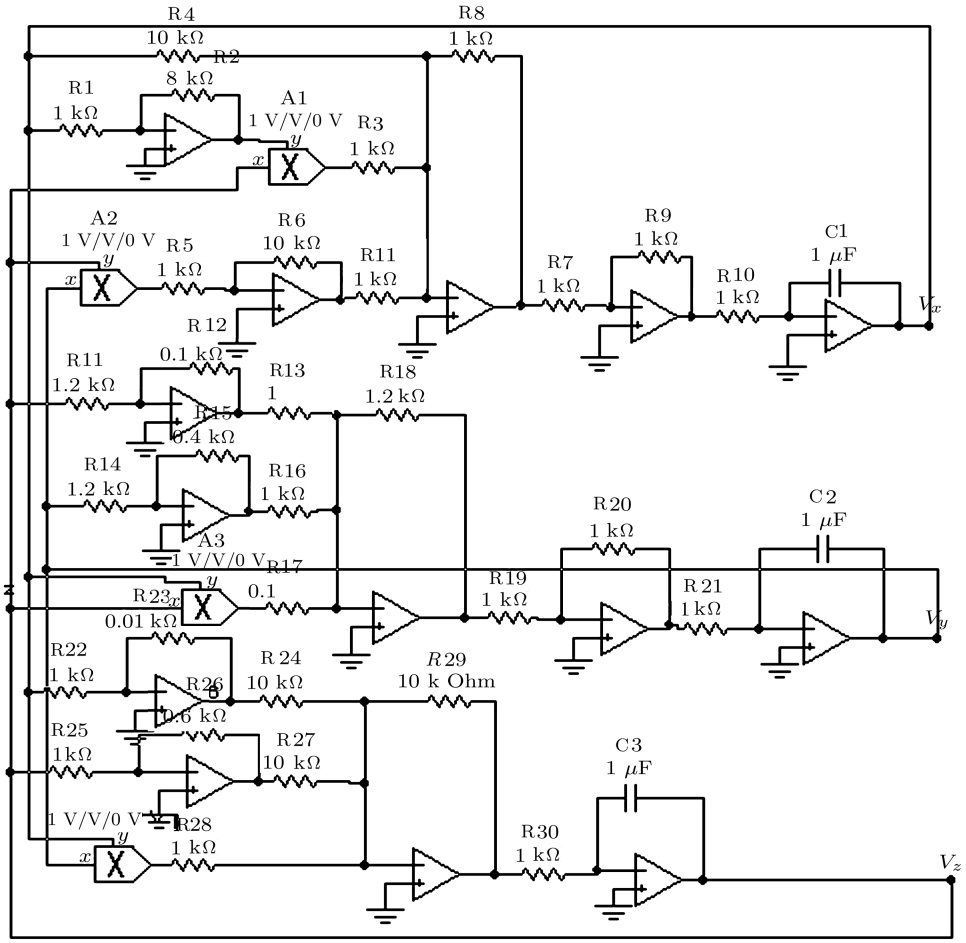


Fig. 10. Circuit diagram for realising the new chaotic system (1): OP-Amps are LM2900 multiplies are AD633.

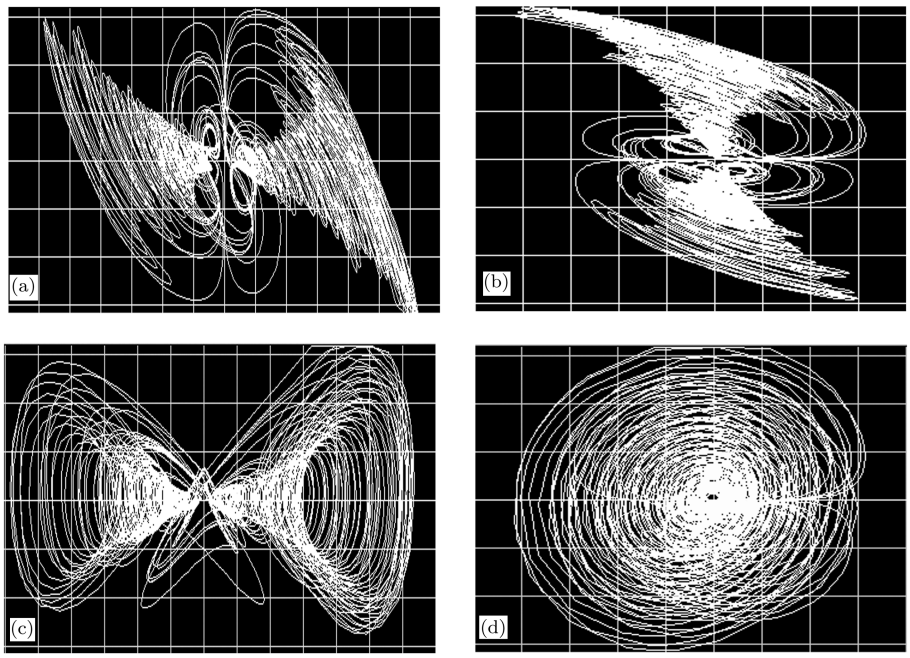


Fig. 11. The phase portraits of new chaotic system observed on the oscilloscope in different planes: (a) x–y plane; (b) y–x plane; (c) x–z plane; (d) y–z plane.

5. Analysis of frequency spectrum

Recently, many schemes of extracting messages masked by chaos have been reported. One of the reasons is that the bandwidth of frequency spectra of chaotic signals is not broad enough.[22−25] The novel system has a broad bandwidth. To compare, only the bandwidths of the signals generated numerically by the system itself are discussed here, without investigating possible electronic techniques that may further improve the bandwidths of such systems. Suppose that the frequency range with spectral values over 10^{-1}, then one can have the broad bandwidths of the different systems. The bandwidths of Lorenz system and Chen system are less than $0-2.5$ Hz and $0-4$ Hz.[22−25] However, when $a=0.5, b=0.6, c=0.5, d=4, f=1, g=6, h=0.1$ and $e=0.48, 0.5, 0.6, 0.85$ are fixed, the corresponding frequency spectra are shown in Figs. 12(a)–12(d). One can see that the frequency properties of the new chaotic system are so abundant in broad ranges. Note that the bandwidths of chaotic signals of novel system are all in about $0-25$ Hz respectively from Figs. 12(a)–12(d) which are nearly 4–5 times wider than that of Lorenz system and Chen system. The broad bandwidth of novel system (1) indicates its great potential for some relevant engineering applications such as secure communications.

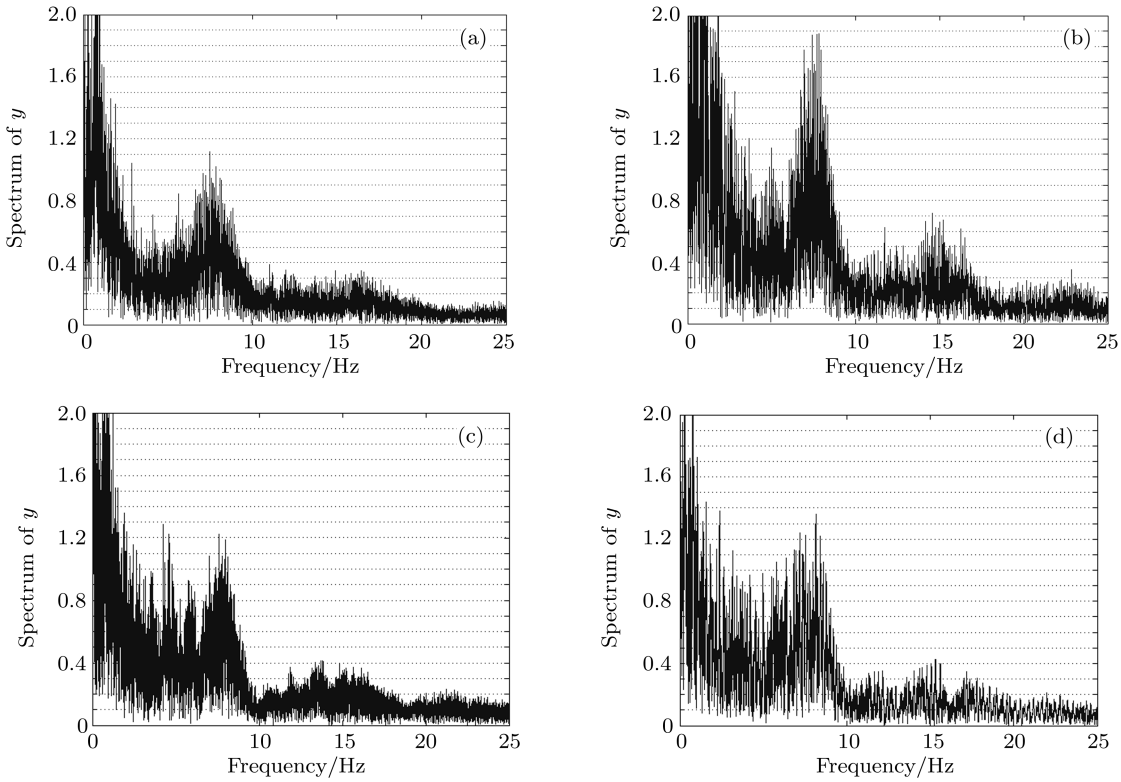


Fig. 12. The frequency spectrum generated numerically from chaotic systems with different parameters: (a) $e=0.48$; (b) $e=0.5$; (c) $e=0.6$; (d) $e=0.85$.

6. Conclusion

This paper introduces a novel 3D autonomous system which has been rarely discussed in previous work. Complex chaotic behaviours of the system are described by phase portraits, Lyapunov exponents, frequency spectrum, etc. The dynamical behaviours of the system are further investigated in physical applications such as electronic circuits, frequency spectrum. The circuit experimental results show the agreement with numerical simulations. Frequency spectrum analysis shows a broad frequency bandwidth, this system has perspective of potential applications in such engineering fields as secure communication.

References

[1] Sparrow C 1982 *The Lorenz Equations* (New York: Springer-Verlag) p112–138

[2] Rosslor O Er 1976 *Phys. Lett.* A **57** 397

[3] Ueta T and Chen G R 2000 *Int. J. Bifur. Chaos* **10** 1917

[4] Chen G R 1999 *Controlling Chaos and Bifurcations in Engineering Systems* (Boca Raton, Fla: CRC Press) p86–89

[5] Zhou T S, Chen G R and Tang Y 2004 *Int. J. Bifur. Chaos* **14** 3167

[6] Lü J H and Chen G R 2002 *Int. J. Bifur. Chaos* **12** 659

[7] Lü J H, Chen G R, Cheng D Z and Celikovsky S 2002 *Int. J. Bifur. Chaos* **12** 2917

[8] Zhou P, Cao Y X and Cheng X F 2009 *Chin. Phys.* B **18** 1394

[9] Qi W and Wang Y H 2009 *Chin. Phys.* B **18** 1404

[10] Qu S X, Lu Y Z, Zhang L and He D R 2008 *Chin. Phys.* B **17** 4418

[11] Zhang C X and Yu S M 2009 *Chin. Phys.* B **18** 119

[12] Wang G Y and He H L 2008 *Chin. Phys.* B **17** 4014

[13] Xu Z and Liu C X 2008 *Chin. Phys.* B **17** 4033

[14] Dong E Z, Chen Z P, Chen Z Q and Yuan Z Z 2009 *Chin. Phys.* B **18** 2680

[15] Zhou P, Wei L J and Chen X F 2009 *Chin. Phys.* B **18** 2674

[16] Liu C X and Liu L 2009 *Chin. Phys.* B **18** 2188

[17] Liu Y Z, Jiang C S, Lin C S and Sun H 2007 *Acta Phys. Sin.* **56** 5131 (in Chinese)

[18] Gao B J, Lu J A and Chen A M 2006 *Acta Phys. Sin.* **55** 4450 (in Chinese)

[19] Luo X H, Zhou W, Li R, Liang Y L and Luo M W 2009 *Chin. Phys.* B **18** 2168

[20] Li C, Liao X and Wong K 2005 *Chaos, Solitons and Fractals* **23** 183

[21] Feki M 2003 *Chaos, Solitons and Fractals* **18** 141

[22] Dong G G, Zheng S, Tian L X, Du R J, Sun M and Shi Z Y 2009 *Phys. Lett.* A **373** 4227

[23] Wang F Z, Qi G Y, Chen Z Q and Yuan Z Z 2007 *Acta Phys. Sin.* **56** 3137 (in Chinese)

[24] Qi G Y, Chen G R, van Wyk M A, van Wyk B J and Zhang Y 2008 *Chaos, Solitons and Fractals* **38** 705

[25] Dong G G and Tian L X 2008 *Phys. Lett.* A **372** 4241